Enhanced automated Alzheimer's disease detection from MRI images by exploring handcrafted and transfer learning feature extraction methods

Touati Menad[1], Mohamed Bentoumi[1], Arezki Larbi[1], Malika Mimi[1], Abdelmalik Taleb Ahmed[2]

[1]Department of Electrical Engineering and Laboratory of Signals and Systems, Faculty of Sciences and Technology, University Abdelhamid Ibn Badis of Mostaganem, Mostaganem, Algeria
[2]Institute of Electronics, Microelectronics and Nanotechnology (IEMN), Université Polytechnique Hauts de France, Université de Lille, Centre National de la Recherche Scientifique (CNRS), Valenciennes, France

Article Info

ABSTRACT

The rising prevalence of Alzheimer's disease (AD) poses a significant global health challenge. Early detection of AD enables appropriate and timely treatment to slow disease progression. In this paper, we propose an enhanced procedure for automated AD detection from magnetic resonance imaging (MRI) images, focusing on two primary tasks: feature extraction and classification. For feature extraction, we have investigated two categories of methods: handcrafted techniques and those based on pre-trained convolutional neural network (CNN) models. Handcrafted methods are preceded by a preprocessing step to improve the MRI image contrast, while the pre-trained CNN models were adapted by utilizing only a part of the models as feature extractors, incorporating a global average pooling (GAP) layer to flatten the feature vector and reduce its dimensionality. For classification, we employed three different algorithms as binary classifiers to detect AD from MRI images. Our results demonstrate that the support vector machine (SVM) classifier achieves a classification accuracy of 99.92% with Gabor features and 100% with ResNet101 CNN features, competing with existing methods. This study underscores the effectiveness of feature extraction using Gabor filters, as well as those based on the adapted pre-trained CNN models, for accurate AD detection from MRI images, offering significant advancements in early diagnosis.

Corresponding Author:

Touati Menad
Department of Electrical Engineering and Laboratory of Signals and Systems, Faculty of Sciences and Technology, University Abdelhamid Ibn Badis of Mostaganem
Route Belahcene.Bp 277, Mostaganem, Algeria
Email: touati.menad.etu@univ-mosta.dz

1. INTRODUCTION

Alzheimer's disease (AD) is a progressive neurodegenerative condition that primarily impacts the brain, resulting in a gradual deterioration of memory, cognitive abilities and social aptitude. From a structural perspective of the brain, AD is characterized by brain shrinkage and eventual neuronal death, rendering it the foremost cause of dementia [1]. AD represents a distinct and pathological condition beyond what is considered normal aging, yet the likelihood of developing AD rises as individuals grow older. Approximately 5% of individuals aged 65 to 74 years are affected by AD, while nearly 50% of those aged 85 and older suffer from

the disease [2]. In 2020, it was estimated that around 50 million people worldwide were living with AD [3], [4]. This number is expected to reach approximately 131.5 million people worldwide by 2050 [5].

The early detection of AD represents one of the most intricate challenges for neurologists. Various brain imaging modalities, including magnetic resonance imaging (MRI), computed tomography (CT), and positron emission tomography (PET), allow for the identification of structural and functional changes associated with AD. However, the manual examination of images by doctors or radiologists is often time-consuming and susceptible to errors. The development of automated diagnostic aid systems provides valuable support to healthcare professionals, facilitating the early detection of AD and enabling quicker and more accurate diagnoses while reducing medical errors and enhancing treatment outcomes.

According to the literature, AD detection methods are based either on a single imaging modality or on multimodal approaches, particularly combining MRI with PET. Multimodal techniques can be categorized into two types: those that fuse features extracted from both imaging modalities [6], [7] and those that merge MRI and PET images [8]–[10]. The latter approach, while requiring highly complex image fusion techniques, is more effective for tracking the progression of AD. However, PET, as an invasive modality involving a radioactive tracer [6], [7], is often less favored compared to MRI alone in the context of AD detection. MRI is the most widely used imaging modality [11] due to its non-invasive nature and its capacity to provide high-resolution structural information about the brain.

In the context of AD detection from MRI images, the process encompasses three key stages: image preprocessing, feature extraction, and classification. The preprocessing steps may include denoising, contrast enhancement, and/or segmentation to detect and localize the region of interest (ROI). Segmentation is particularly beneficial for the detection and identification of brain tumors [12]. However, in the context of Alzheimer's disease detection, segmentation is not strictly necessary, as AD affects the entire brain. Nonetheless, it becomes relevant when applying methods for extracting morphological features from the brain [13]. Feature extraction is a transformation operation that converts an image (2D) into a feature vector (1D) that represents its information. Feature extraction methods are generally classified into handcrafted methods and CNN-based methods. The classification step assigns observations to predefined categories or classes based on their feature vectors.

In this paper, we present an enhanced procedure for automated AD detection from MRI images. Our approach comprises two primary steps: feature extraction and classification. For feature extraction, we investigate several methods: three handcrafted methods (histogram of oriented gradients (HOG), local binary patterns (LBP) and Gabor filters) and nine pre-trained CNN models [14] (VGG16, AlexNet, ResNet101, GoogLeNet, DenseNet, InceptionV3, SqueezeNet, MobileNetV2 and ShuffleNet). Handcrafted methods are preceded by a filtering-based pre-processing step to improve MRI image quality before applying the extractors. The pre-trained CNN models are adapted by adding a global average pooling (GAP) layer without fine-tuning the network parameters. For the classification step, we employed three classifiers: support vector machine (SVM), k-nearest neighbors (KNN) and decision trees (DT). These classifiers are used to distinguish between Alzheimer's disease (AD) and normal cases (cognitively normal, CN) classes from MRI images. Our results are compared with those presented in related works.

Our major contributions in this paper are summarized as
− We explored two approaches for feature extraction from MRI images: the handcrafted approach and the transfer learning (TL) approach.
− We utilized three classifiers—SVM, KNN, and DT—to classify AD and CN subjects, enabling us to identify the optimal combination of feature extractor and classifier.
− We used three publicly available databases containing MRI images via the Kaggle platform.
− To assess the generalization ability of each extractor-classifier combination, we applied k-fold cross-validation.

The remainder of the paper is organized as follows. Section 2 reviews related work in the field of AD detection from MRI images. Section 3 details the proposed methodology, outlining the various steps involved. In section 4, we present the experimental setup and results, followed by a discussion comparing our findings with state-of-the-art methods. Finally, section 5 concludes the paper.

2. RELATED WORK

Automatic detection and diagnosis of Alzheimer's disease (AD) are major challenges in the field of neural medical research. In this context, several researchers have presented various models and approaches for the automatic detection and diagnosis of AD from MRI images. Li and Yang [15] used MRI images from

the Alzheimer's disease neuroimaging initiative (ADNI) database for two types of subjects, AD and CN. Three machine learning-based classifiers were employed to predict Alzheimer's disease and identify the regions of the brain affected by this disease. A comparison study was conducted among the three distinct classifiers: SVM, VGGNet and ResNet. The accuracy values for the AD to CN data classification across the three classifiers were: support vector machine (90%), VGGNet (95%), and ResNet (95%). Zhang *et al.* [16] extracted two types of features from MRI images: gray matter (GM) volume and lateralization index (LI), using hypothesis testing. The study included four data classes from the ADNI database: CN, early mild cognitive impairment (EMCI), late mild cognitive impairment (LMCI) and AD. Subsequently, several classification algorithms were employed, including random forest (RF), decision tree (DT), k-nearest neighbor (KNN) and support vector machine (SVM) with linear, RBF and polynomial kernel. For two groups of subjects—AD group versus CN—the SVM classifier with a linear kernel and the KNN classifier achieved the highest accuracies of $98,09\%$ and $98,25\%$, respectively.

Arafa *et al.* [17] applied deep learning (DL) to detect and diagnose AD using two convolutional neural network models: a custom end-to-end CNN developed from scratch and a fine-tuned VGG16 model. The implementation involved three stages: dataset preparation with image size reduction, data augmentation, and model training/testing with an $80\%/20\%$ split. Evaluation on a subset of MRI images from the ADNI database revealed that the custom CNN achieved an accuracy of 99.95%, while the VGG16 model attained 97.44%. Naz *et al.* [18] employed machine learning (ML) and deep learning to detect and identify Alzheimer's disease. They proposed a system of CNN-based architectures using features extracted from MRI images of the entire ADNI database, which contains three different class types (AD, CN and mild cognitive impairment (MCI)). The classification was performed out by the SVM classifier on the three classes distributed as follows: AD/MCI, CN/MCI, and AD/CN. The results reached an accuracy of 99.27% (MCI/AD), 98.89% (AD/CN), and 97.06% (MCI/CN). The CNN-based approach was also utilised by Yousry AbdulAzeem *et al.* [19] on the ADNI database containing two-class MRI images AD and CN. A data augmentation technique was employed to increase the number of data. Feature extraction and classification were performed using an end-to-end CNN, with cross-validation allocating 85% of the data for training, 10% for validation, and 5% for testing. The achieved classification accuracy for AD/CN was 97.80%.

Ismail *et al.* [20] implemented a multimodal image fusion method to merge MRI images with a modular set of image pre-processing procedures. This method was applied to the ADNI database, which includes two classes: AD and CN. To extract relevant and generic information from the fused images, a 3D CNN network was utilized. The characteristics of both classes were classified using three classifiers: CNN, SVM and RF. The AD/CN classification yielded accuarcy values of 98.21%, 91%, and 85.90%, respectively. Rangaraju *et al.* proposed in their research paper [21] an end-to-end CNN model for the automatic identification of Alzheimer's disease using 3D brain MRI data. The model comprises three main components: First, a patch convolutional neural network (PCNN) is employed to extract discriminative features from each MRI patch. Second, an octave convolution layer is utilized to reduce spatial redundancy and expand the receptive field for capturing detailed brain structure. Finally, a dual attention-aware convolutional classifier further refines the feature representation to enhance the accuracy of AD detection. It is worth noting that the MRI data is pre-processed, which includes image scaling and denoising. The designed end-to-end CNN model achieved a test accuracy of 99.87% for categorizing dementia stages using the publicly available Alzheimer's disease neuroimaging initiative (ADNI) dataset.

Referring to Table 1, it is evident that there are still improvements to be made in the automation process for detecting Alzheimer's disease from MRI images. In previous works based on DL methods, convolutional neural network models have often been trained or fine-tuned on small image databases. However, convolutional neural networks require large datasets (big data) for effective learning. To address this limitation, we propose to use pre-trained CNN models as feature extractors without readjusting the network parameters. Moreover, our work distinguishes itself through the application of Gabor filters as feature extractors on MRI images for AD detection. To our knowledge, this is the first study to investigate this approach, thereby opening new perspectives in the field of biomedical image analysis. Furthermore, another significant motivation behind our work is to propose a straightforward and accessible procedure that circumvents the use of complex methods, such as those based on multimodal or 3D MRI analysis. By simplifying the tools employed, we aim to enhance detection efficiency while ensuring greater applicability in clinical settings where resources and time are often constrained.

Table 1. Summary of the state-of-the-art for AD detection

Authors and references	Feature extractor	Database	Classification method	Cross-validation	Accuracy (%)
Li and Yang (2021) [15]	CNN	AD-CN (ADNI) dataset	SVM(TL)	85% training and 15% test	90
			3D-VGGNet (end to end)		95
			3D-ResNet (end to end)		95
Zhang *et al.* (2022) [16]	GM	AD-CN-MCI (ADNI) dataset	SVM	10-fold	98.09
	LI		RF		94.60
	GM+LI		DT		91.10
			KNN		98.25
Arafa *et al.* (2023) [17]	CNN	AD-CN (ADNI) dataset	CNN (end to end)	80% training and 20% test	99.95
			VGG16 (end to end)		97.44
Naz. *et al.* (2021) [18]	AlexNet(conv5)	AD-CN-MCI (ADNI) dataset	SVM	80% training, 10% validation and 10% test	91.38
	VGG16(FC6)		KNN		98.89
	VGG19(FC6)				99.27
AbdulAzeem *et al.* (2021) [19]	CNN	AD-CN (ADNI) dataset	CNN (end to end)	95% training and 5% test	97.80
Ismail *et al.* (2022) [20]	CNN	AD-CN (ADNI) dataset	SVM	10-fold	91.00
			RF		85.90
			3D CNN (end to end)		98.21
Rangaraju *et al.* (2024) [21]	CNN	EMCI-LMCI-MCI-AD-CN (ADNI) dataset	3D-CNN (end to end)	Holdout	99.87

3. DESCRIPTION OF THE METHODOLOGY

In this paper, we propose an enhanced automated procedure for AD detection using machine learning techniques applied to an MRI image dataset, aiming to achieve high-performance results in the AD detection. The proposed procedure can be divided into two key phases: feature extraction and classification. We explored two approaches for feature extraction from MRI images: the handcrafted approach and the transfer learning (TL) approach [22].

As illustrated in Figure 1, the procedure is divided into two distinct pipelines, each corresponding to the implementation of one of the considered approaches for feature extraction. The handcrafted approach involves a two-step process. First, the input image is filtered to improve its contrast. Subsequently, feature extraction transforms the filtered images into feature vectors. We explored three handcrafted methods: HOG, LBP, and Gabor methods. On the other hand, the transfer learning approach uses pre-trained CNN models as feature extractors.

Finally, a classification process is performed on the feature vectors using three different classifiers: SVM, KNN, and decision tree (DT). In the following paragraphs, a brief overview of all these methods is provided, preceded by a short description of the MRI image datasets used in this work.
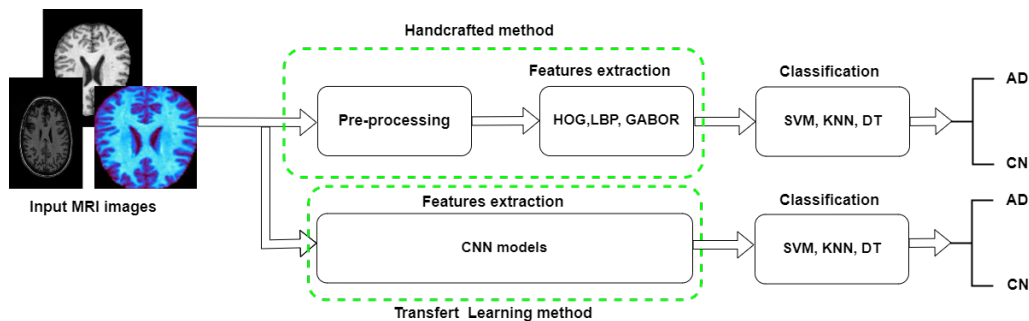

Figure 1. Block diagram of the proposed framework

3.1. Description of the databases

The first crucial stage in a machine learning process is data collection. The quality of the training data is essential to ensure the accuracy of predictions made by machine learning systems. In this work, we have used

three publicly available databases from the Kaggle platform, each one with an unbalanced distribution of MRI images. The first database contains 5121 images of 176×208 pixels, divided into four classes: *NonDemented, MildDemented, ModerateDemented,* and *VeryMildDemented*. The second database consists of 6163 images of dimensions $369 \times 369 \times 3$ divided into three categories: *NonDemented, MildDemented,* and *VeryMildDemented*. The third database, known as the Alzheimer's disease neuroimaging initiative (ADNI) entails 5154 images of varying sizes (170×256, 166×256, and 160×260 pixels) and comprises three classes: Alzheimer's disease (AD), mild cognitive impairment (MCI) and cognitively normal (CN). To evaluate our proposed method, we have combined some categories from the three databases into two distinct labels, Alzheimer's disease (AD) and normal cases (cognitively normal, CN) for AD detection. The selection given includes 400 images from each database divided into 200 AD images and 200 CN images. Thus, the final dataset consists of 1200 grayscale 2D MRI images with two distinct categories: 600 AD images and 600 CN ones. All images are resized to (256×256) pixels to ensure size uniformity, as reported in Table 2.

Table 2. Distribution of selected MRI images from the three databases.

Database and format	Labeling	# of images	Size of images
Database 1 (MRI images) format JPEG	Cognitively Normal (CN)	200	256×256
	Alzheimer's disease (AD)	200	
Database 2 (MRI images) format JPEG	Cognitively Normal (CN)	200	256×256
	Alzheimer's disease (AD)	200	
Database 3 (MRI images) ADNI format PNG	Cognitively Normal (CN)	200	256×256
	Alzheimer's disease (AD)	200	

3.2. Feature extraction

The feature extraction phase in an automated Alzheimer's disease (AD) detection procedure using MRI images is crucial, as the quality of the features directly impacts the performance of the process. This phase can be considered as a transformation process from a 2D image to a 1D vector, where each element of the vector represents a relevant feature of the image. In proposed work, we have explored several feature extraction methods belonging to two categories of approaches, as previously mentioned. This represents the first suggested main contribution. The following paragraphs present the methods used in this phase.

3.2.1. Handcrafted extractors

The handcrafted methods are applied following a pre-processing step that involves filtering. This step is crucial for improving the initial quality of MRI images by reducing noise and enhancing contrast which allows the handcrafted feature extraction methods to be more effective. In our work, we have opted to use a median filter [23], [24] on the MRI images due to its balance of simplicity and effectiveness. The median filter is particularly well-suited for medical imaging as it effectively removes noise while preserving edges, which are vital for maintaining the integrity of the image structures. The enhanced image quality directly contributes to the robustness and accuracy of the entire detection procedure based on handcrafted feature extraction methods. Subsequently, we have applied handcrafted feature extraction methods. In this work, we have utilized well-known methods, namely the histogram of oriented gradients (HOG) [25], local binary patterns (LPB) [26] [27], and Gabor filters [28], which are introduced next.

a. Histogram of oriented gradients

The histogram of oriented gradients (HOG) [25] is a feature extraction operator used for object detection in images. The HOG descriptor quantifies and represents the textures and shapes present in an image. For each pixel, the intensity gradient is calculated in both horizontal and vertical directions, as shown by (1):

$$\begin{aligned} G_x &= \frac{\partial I(x,y)}{\partial x} \\ G_y &= \frac{\partial I(x,y)}{\partial y} \end{aligned} \tag{1}$$

Where I is the image, G_x is the gradient in the horizontal (x) direction and G_y is the gradient in the vertical (y) direction. In practice, these gradients can be approximated using convolution filters such as the Sobel filter [29].

These gradients are then converted into magnitudes and orientations. The image is divided into small cells, typically 8×8 pixels. For each cell, a histogram of gradient orientations is constructed with the gradients weighted by their magnitudes, the cells are then grouped into blocks (e.g., 2×2 cells). The histograms of the cells within a block are normalized which helps to make the descriptor less sensitive to changes in lighting. Finally, the normalized histograms of all the blocks are concatenated to form a feature vector representing the entire image.

b. Local binary patterns

The LBP method is a technique for extracting texture features from images [26], [27]. Its fundamental principle involves comparing pixel intensities. For each pixel in an image, the method compares the intensity of the pixel with that of its neighboring pixels, typically within a 3×3 neighborhood in Figure 2. If a neighbor's intensity is greater than or equal to the central pixel's intensity, a 1 is assigned; otherwise, a 0 is assigned. This binary comparison is performed for each neighbor, thereby forming a binary pattern around the central pixel.
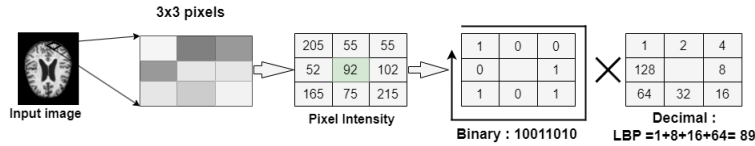
Figure 2. An example of calculating an LBP value

These binary bits are then combined to form an 8-bit binary number in the case of a 3×3 pixel neighborhood. This number is converted into a decimal value, representing a unique LBP pattern. To construct the image's feature vector, a histogram of the occurrences of these decimal values is constructed. This histogram represents the texture patterns present in the image and serves as features of the original image.

c. Gabor filters

Gabor filters is a technique employed as feature extraction method in image processing to extract textural and structural information from images. The process of designing a feature vector using Gabor filters involves several key steps [28], [30]. First, Gabor filters are constructed using sinusoidal functions modulated by a Gaussian function, as described by (2) and (3):

$$G(x, y; \sigma, \theta) = \exp\left(-\frac{x^2 + y^2}{2\sigma^2}\right) \cdot \cos\left(2\pi\frac{x}{\lambda}\right) \tag{2}$$

with:

$$\begin{aligned} x &= m\cos\theta + n\sin\theta \\ y &= -m\sin\theta + n\cos\theta \end{aligned} \tag{3}$$

where m and n are the coordinates of a pixel in the image with size (M, N). The parameter σ controls the scale of the filter, while θ controls its orientation. For each combination of scale σ and orientation θ, we obtain a distinct Gabor filter. Next, each Gabor filter is applied to the image, producing a filtered image, which results in a series of feature maps corresponding to each filter in Figure 3.

The feature vector can then be constructed in various ways. One approach is to calculate global statistics, such as the mean or variance of the filter responses. Alternatively, the responses can be directly concatenated, or histograms of the responses can be created to capture their distribution. Finally, the feature vector is often normalized to ensure that the values are comparable and to minimize the effects of scale or lighting variations. This feature vector is subsequently used for classification tasks.
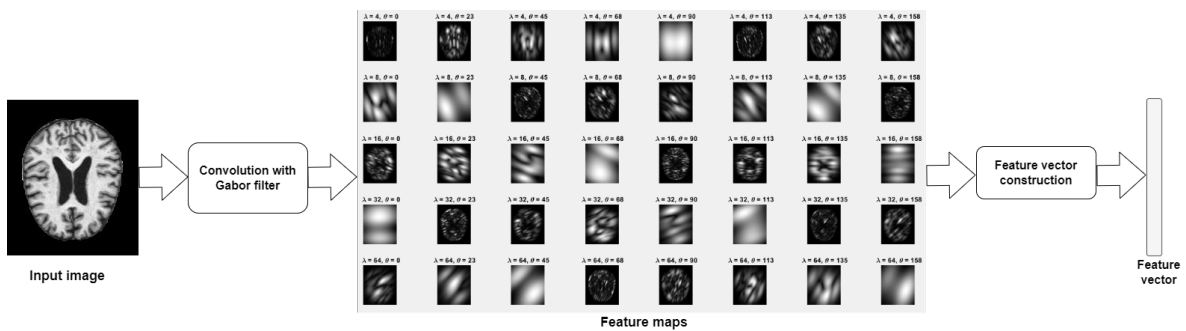

Figure 3. An example of a Gabor filter response with 5 scales and 8 orientations for an MRI image

3.2.2. CNN extractors

For the transfer learning method, we have used nine distinct pre-trained CNN models: AlexNet, ResNet101, DenseNet201, GoogLeNet, SqueezeNet, InceptionV3, VGG16, MobileNetV2, and ShuffleNet [31]. These models were pre-trained on the extensive ImageNet database [32] which comprises over 14 million images distributed across 1,000 different classes. Each CNN model consists of two main parts: a feature extraction part and a classification part as shown in Figure 4.
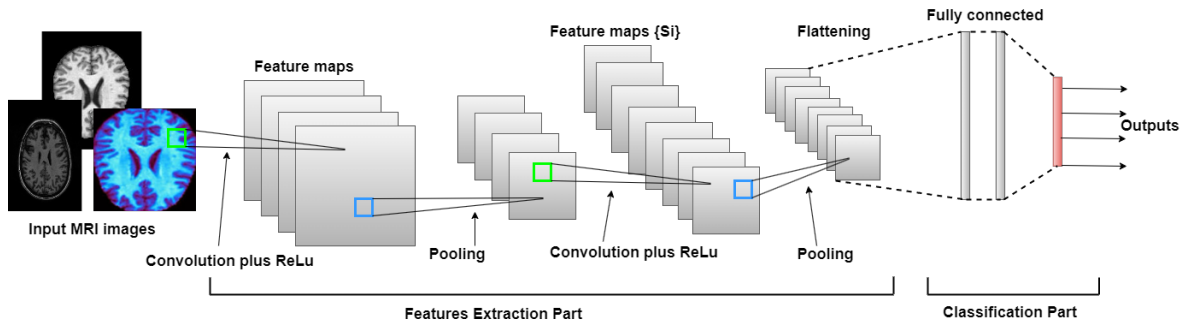

Figure 4. An example of CNN network architecture

The feature extraction part is composed of a series of blocks. Each block includes convolutional layers that extract hierarchical features from the input images, as well as pooling layers to reduce dimensionality. The feature maps produced by these blocks are then processed by a nonlinear activation function, such as the rectified linear unit (ReLU) [12], [33]. The classification part consists of fully connected (FC) layers with the last FC layer employing the Softmax function for classification.

In our work, we have utilized the nine pre-trained models mentioned earlier within the transfer learning (TL) framework to efficiently extract feature vectors from MRI images. This approach avoids the need to design new CNN models from scratch which requires a large database and significant computational resources. We have carefully adapted these models to enhance performance and to reduce both the cost and training time required. Specifically, based on prior work [33], we identified and removed the classification component and the final pooling layer from the feature extraction part of each pre-trained CNN model. As a result, at the output of the remaining feature extraction section, we obtained a set of feature maps $\{S_i\}$ with dimensions M and N, which depend on the characteristics of the last convolutional layer for each pre-trained CNN model. Flattening this set of features to create a feature vector results in a very high dimensionality. Therefore, to enhance classification performance, it was necessary to reduce the dimensionality of the feature vectors by incorporating a global average pooling layer into the retained part of each pre-trained CNN model. This operation flattens and reduces the size of the feature vectors in a single step as shown in Figure 5. The global average pooling (GAP) is described as (4):

$$x_i = \frac{\sum_m^M \sum_n^N S_i(m,n)}{M \times N}; i \in [1, p] \tag{4}$$

Where (M, N) are the size of the last p feature maps $\{S_i\}$ from the retained part. These results in a feature vector X of dimension p for each image, regardless of its size. This method does not require retraining or fine-tuning the pre-trained CNN models. The obtained feature vectors are then used in the subsequent procedure for detecting Alzheimer's disease (AD) from MRI images.
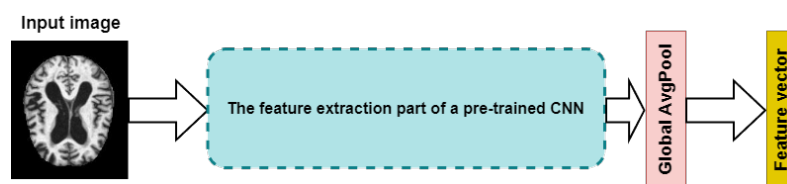

Figure 5. Pre-trained models used for feature extraction

3.3. Classification

Detection of Alzheimer's disease from MRI images is regarded as a binary classification problem (positive class: AD and negative class: CN). Classification can be based on either supervised or unsupervised methods. When we have labeled data (labeled observations), we are addressing a supervised classification problem, as is the case in this work. Conversely, if the data is unlabeled, it would represent an unsupervised classification scenario. In our study, we employed three supervised classification methods for binary classification: support vector machine (SVM) [34], [35], k-nearest neighbors (KNN) [36] and decision tree (DT) [37] which are briefly introduced in the following paragraphs.

a. Support vector machine (SVM) classifier

A support vector machine (SVM) is a machine learning algorithm introduced by Vladimir Vapnik [34]. SVM aims to find an optimal linear hyperplane separating two classes. Its principle is based on maximizing the margin between the data distributions of the two classes in the feature space (the distance between the two classes) while minimizing classification errors [38]. For an SVM classifier, we consider a training set D consisting of N examples (X_i, y_i) with $X_i \in R^p$ belonging to one of the two classes and labeled by $y_i \in \{+1, -1\}$. The separating hyperplane H can be defined by equation (2), where $w \in \mathbb{R}^p$ and $b \in \mathbb{R}$ represent the parameters of the separating hyperplane.

$$H : \langle w, X_i \rangle + b \tag{5}$$

The values of w and b are determined through learning by minimizing the criterion J (eq. 3.3.) under the following constraints:

$$\begin{aligned} &\min_{w,b} J = \tfrac{1}{2}w^2 \\ &\text{under the constraints:} \\ &y_i\left(\langle w, X_i \rangle + b\right) \geqslant 1 \;\; ; i = 1 \cdots N \end{aligned} \tag{6}$$

b. The k-nearest neighbor (KNN) classifier

The k-nearest neighbor (KNN) classifier is a non-parametric supervised learning algorithm that classifies data based on the proximity of points in the feature space. Initially developed by Evelyn Fix and Joseph Hodges in 1951, and later extended by Thomas Cover in 1967, KNN operates by identifying the k nearest neighbors of a data point to be classified, using a distance measure, often Euclidean distance. KNN then assigns the majority class among these neighbors to the data point in question. The method consists of two main steps: determining the nearest neighbors and assigning the class based on these neighbors.

c. Decision tree (DT) classifier

The decision tree is a supervised learning algorithm used for classification and is often applied to image feature vectors. It builds models in a tree structure where each node represents a test on a feature of the input. The branches of the tree correspond to possible values of the attributes, while the leaves denote the final decisions or predicted classes. The decision tree recursively partitions the data space based on evaluation criteria to select the best splitting features, employing heuristics to prevent overfitting. This model effectively classifies data by constructing a series of tests based on numerical attributes compared to predefined thresholds.

4. EXPERIMENTATION AND RESULTS

The objective of this work is to develop an automated procedure for detecting Alzheimer's disease from MRI images. As previously mentioned, this procedure consists of two main phases: feature extraction and classification. To design and evaluate it, we followed a series of steps outlined in the flowchart shown in Figure 6. The source code for this methodology was developed within the MATLAB environment.

First, we constructed an MRI image database by merging three distinct datasets, as detailed in section 3.1. These publicly available datasets from Kaggle differ in image quality, dimensions and classes. Images originally in color were converted to grayscale, and then resized to 256×256 pixels to ensure uniformity. We randomly selected 400 images from each dataset, with 200 images per category (AD and CN), ensuring that the final merged dataset maintains high quality and is free from notable artifacts. This process resulted in a database comprising 1200 MRI images, evenly divided into two classes: 600 images in the AD class (positive class) and

600 images in the CN class (negative class). We then applied feature extraction methods to all the images in this database, utilizing three handcrafted methods as well as nine pre-trained CNN models, each serving as a feature extractor as shown in Figure 6. The handcrafted methods are preceded by a pre-processing step based on filtering to enhance the quality of the MRI image, while the pre-trained CNN models have only been adapted by the addition of a global average pooling (GAP) layer without any fine-tuning network parameters.
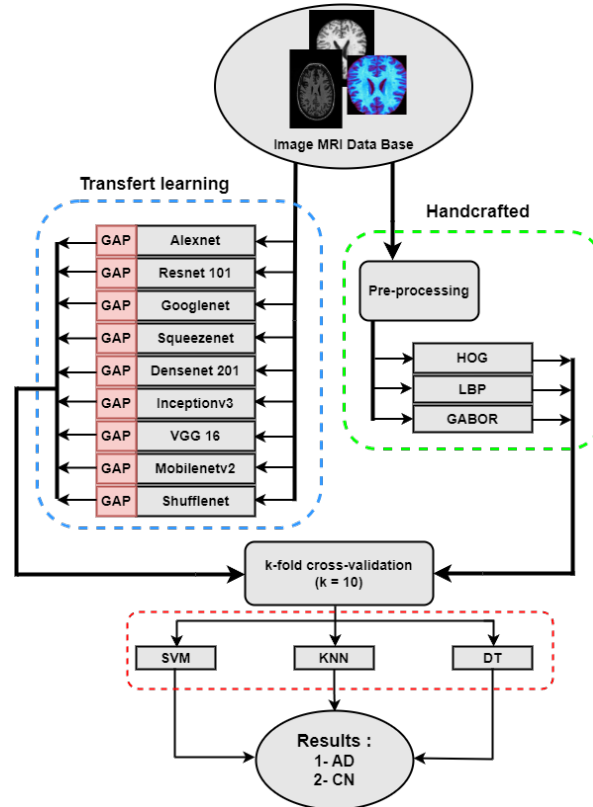
Figure 6. Detailed synoptic of the different stages of the work process

Next, we examined all possible combinations of feature vectors by pairing them with three classifiers: SVM, KNN, and DT. This resulted in 36 different combinations, enabling a thorough evaluation of the implemented procedure. To assess the performance of these combinations, and consequently the overall procedure for detecting AD from MRI images, we have employed several metrics, which will be detailed in the following subsection.

4.1. Performance metrics and validation

To objectively evaluate the performance of our procedure, we use several key metrics: accuracy (ACC), sensitivity (SEN), and specificity (SPE). These metrics are calculated by comparing our predicted outputs with the actual data. The classification results are categorized into four types: true positive (TP), true negative (TN), false positive (FP), and false negative (FN) [38]. The metrics are defined as follows:

− Accuracy (ACC) is calculated by the formula:

$$ACC = \frac{TP + TN}{TP + TN + FP + FN} \qquad (7)$$

− Sensitivity (SEN) is given by:

$$Sensitivity = \frac{TP}{TP + FN} \qquad (8)$$

− Specificity (SPE) is computed using:

$$\text{Specificity} = \frac{TN}{TN + FP} \tag{9}$$

These metrics are employed to assess the performance of the SVM, KNN, and DT classifiers. In this study, we estimate these performance metrics using the k-fold cross-validation method [33] [37]. The dataset is divided into k subsets. We train the model on $k-1$ of these subsets while testing (i.e., evaluating performance metrics) on the remaining subset. This process is repeated k times, with each subset serving as the test set once. The global accuracy (GA) is the average of the performance metrics obtained across all k iterations, calculated as (10):

$$\text{GA} = \frac{1}{k} \sum_{i=1}^{k} \text{ACC}_i \tag{10}$$

Similarly, the average sensitivity (G_{sen}) and average specificity (G_{spe}) are computed across all k iterations, calculated as (11):

$$G_{\text{sen}} = \frac{1}{k} \sum_{i=1}^{k} \text{SEN}_i \tag{11}$$

$$G_{\text{spe}} = \frac{1}{k} \sum_{i=1}^{k} \text{SPE}_i \tag{12}$$

We apply ten-fold cross-validation ($k = 10$) to evaluate our proposed procedure.

4.2. Results and analysis

In this subsection, we present the main results obtained through our procedure for detecting Alzheimer's disease from MRI images. It is important to emphasize that the primary objective of this procedure is to distinguish between images representing Alzheimer's disease (AD) and those of normal cases (cognitively normal, CN). Table 3, along with Figures 7 to 9, provides a comparison of classification performance using various combinations of feature extractors and classifiers.

Among the handcrafted features used, Gabor features combined with the SVM classifier achieved the best overall performance, with an accuracy (GA) of 99.92%, sensitivity (G_{sen}) of 99.83%, and specificity (G_{spe}) of 100%. Although LBP and HOG features also exhibited good performance, their results were slightly lower compared to the other features. LBP and HOG feature extraction methods are particularly effective at capturing local texture patterns; however, this may not be sufficient to address the complexity of MRI images in the context of AD detection.

Among the pre-trained CNN models tested, ResNet101 demonstrated exceptional performance, achieving a 100% accuracy when combined with the SVM classifier. Other models, such as DenseNet201, SqueezeNet, and AlexNet, also exhibited excellent performance, with accuracy rates exceeding 99% in most cases, particularly when paired with the SVM classifier. In contrast, features extracted using the VGG16 model showed relatively weaker performance in comparison. Specifically, the VGG16 model combined with the DT classifier produced modest results, with global accuracy, global sensitivity, and global specificity all rated at 91.33%.

Regarding the classifiers, the SVM proved to be the most effective when combined with various feature extractors, including pre-trained CNN models, achieving the highest scores in overall accuracy, sensitivity, and specificity. The KNN classifier also demonstrated solid performance, though it was slightly less effective than the SVM. However, KNN outperformed SVM when used with Gabor and DenseNet201 feature extractors. In contrast, the DT classifier showed more variable results, with accuracy rates sometimes falling below 95%, making it less effective compared to the SVM and KNN classifiers.

4.3. Comparison with state-of-the-art methods

In this subsection, we compare the performance of our enhanced procedure with that of related works for Alzheimer's disease detection. It is crucial to note that providing comparisons to other related works is challenging due to the differing protocols and image databases used for assessment. To ensure a fair comparison, we focused on studies that closely align with our context, specifically those employing a single imaging

modality (MRI) and utilizing the ADNI database. Additionally, we have focused on binary classification performance results (AD vs. CN) to maintain consistency. While our results are promising, further research, including statistical analysis, may be required to validate these findings and to explore more effective methods for enhancing robustness and accuracy in Alzheimer's disease detection.

Table 3. Comparison of classification performance for the proposed framework

| Extractors	Classifiers	Classification performance (%)		
		GA	G_{sen}	G_{spe}
GABOR	SVM	99.92	99.83	100
	KNN	99.75	100	99.5
	DT	94.33	94	94.67
LBP	SVM	91.42	92.5	90.33
	KNN	99	98.83	99.17
	DT	91.33	92.83	89.83
HOG	SVM	95.25	92.83	97.67
	KNN	99.17	99.33	99
	DT	91.5	91.17	91.83
Alexnet	SVM	99.83	99.83	99.83
	KNN	98.92	98.33	99.5
	DT	96.25	96	96.5
Googlenet	SVM	99.17	99.17	99.17
	KNN	98.58	98.5	98.67
	DT	94.25	93	95.5
Resnet101	SVM	100	100	100
	KNN	99.58	99.83	99.33
	DT	94.58	95	94.17
Squeezenet	SVM	99.75	99.83	99.67
	KNN	99.33	99.67	99
	DT	95.58	95.17	96
Densenet201	SVM	99.75	99.83	99.67
	KNN	99.58	99.5	99.67
	DT	97.08	97.17	97
Inceptionv3	SVM	99.58	99.5	99.67
	KNN	99.33	99.67	99
	DT	93.67	94	93.33
VGG16	SVM	98.83	98.83	98.83
	KNN	98.25	98	98.5
	DT	91.33	91.33	91.33
Mobilenetv2	SVM	99.67	99.67	99.67
	KNN	99.33	99.86	98.83
	DT	92.67	91.83	93.5
Shufflenet	SVM	99.58	99.5	99.67
	KNN	99.08	99.17	99
	DT	93.83	94.67	93
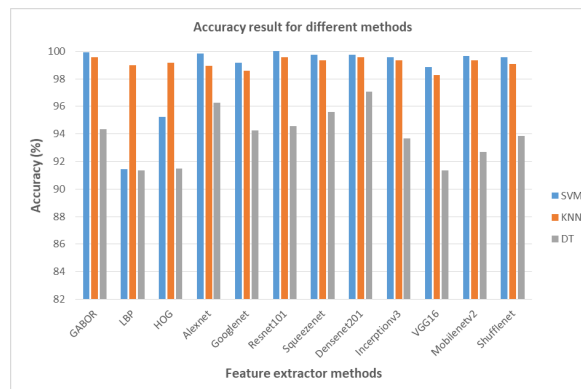
Figure 7. Global accuracy for each classifier combined with various feature extractors
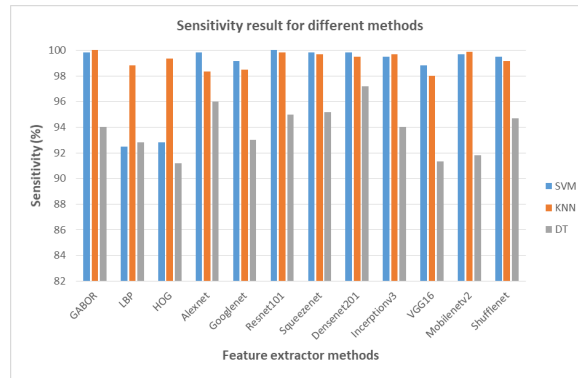
Figure 8. Global sensitivity for each classifier combined with various feature extractors
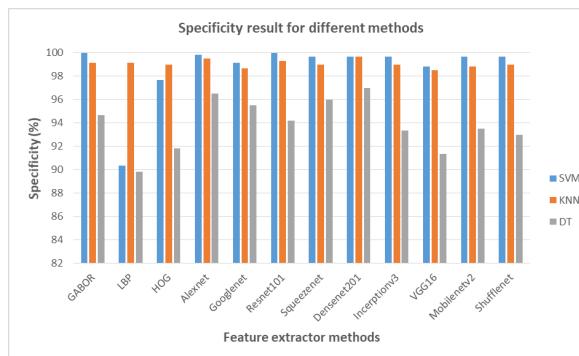

Figure 9. Global specificity for each classifier combined with various feature extractors

According to Table 4, our method competes with, and even surpasses, the results obtained from other techniques in classifying AD and CN subjects. The ResNet101 model, combined with the SVM classifier, achieved a perfect accuracy of 100%. This is mainly attributed to the adaptation of the pretrained CNN model for the feature extraction task. This adaptation enables the extraction of relevant feature vectors, allowing the SVM algorithm to find an optimal separator between the two classes by maximizing the margin in the feature space. On the other hand, the method based on Gabor filter feature extraction exhibited impressive performance. This is mainly because the Gabor filter extraction involves varying scales and orientations of the filter (see subsection 3.2.1.), which allows for the extraction of significant features from MRI images. These features enable the SVM classifier to effectively distinguish between the two classes.

Table 4. Comparison of our proposed framework to other state-of-the-art techniques

Authors	Extractors	Classifiers	Accuracy %
Qi Li *et al.* [15]	CNN	ResNet (end to end)	95
		SVM	90
Arafa *et al.* [17]	CNN	VGG16 (end to end)	97.44
AbdulAzeem *et al.* [19]	CNN	CNN (end-to-end)	97.5
		SVM	91.00
Ismail *et al.* [20]	CNN	RF	85.90
		3D-CNN (end to end)	98.21
Rangaraju *et al.* [21]	CNN	3D-CNN (end to end)	99.87
Proposed framework	Gabor	SVM	99.83
	CNN(ResNet101)	SVM	100

5. CONCLUSION

In this study, we developed an automated framework for detecting Alzheimer's disease (AD) from MRI images by examining various feature extraction techniques and classification methods. Our approach

involves investigating handcrafted methods and pre-trained CNNs as feature extractors with different classifiers to achieve robust detection performance. Among the handcrafted features, Gabor features combined with the SVM classifier reached the highest performance, achieving an accuracy of 99.92%. This indicates that the Gabor filter-based method is particularly well-suited for extracting texture information from MRI images relevant to AD detection. On the other hand, the ResNet101 pretrained CNN model paired with SVM achieved a perfect accuracy of 100%, showcasing its efficiency in feature extraction from MRI images. This success is primarily due to the effectiveness of the proposed adaptation of the pre-trained CNN model for feature extraction, which allows to provide highly relevant feature vectors. These vectors empower the SVM algorithm to identify an optimal separator between the two classes in the feature space by maximizing the margin between them. Moreover, the SVM classifier consistently demonstrated the highest overall accuracy across all feature extractors when compared to the KNN and DT classifiers.

Our approach exhibits competitive performance relative to related methods for Alzheimer's disease detection, highlighting the robustness of our framework and its potential in the field of AD detection from MRI images. While our results are promising, additional research considering comprehensive statistical analysis is necessary to validate these findings and ensure their reliability. Furthermore, the dataset used in this study, while substantial, may not fully capture the diversity of MRI images across various populations and stages of Alzheimer's disease. To enhance generalizability, future work should aim to expand the dataset to include a broader range of images representing different demographics and disease stages.

Furthermore, while handcrafted features such as Gabor features have shown strong performance, relying solely on these methods may restrict the system's adaptability to novel or unseen MRI data. Future research should investigate advanced or hybrid feature extraction techniques that integrate both handcrafted methods and transfer learning with CNN models to improve adaptability and performance. Finally, efforts should concentrate on refining feature extraction methods and improving computational efficiency to further advance automated Alzheimer's detection from MRI images.

REFERENCES

[1]   D. S. Knopman *et al.*, "Alzheimer disease," *Nature Reviews Disease Primers*, vol. 7, no. 1, p. 33, May 2021, doi: 10.1038/s41572-021-00269-y.

[2]   M. F. Mendez, "Early-onset Alzheimer's disease: nonamnestic subtypes and type 2 AD," *Archives of Medical Research*, vol. 43, no. 8, pp. 677–685, 2012, doi: 10.1016/j.arcmed.2012.11.009.

[3]   I. T. Lott and E. Head, "Dementia in down syndrome: unique insights for alzheimer disease research," *Nature Reviews Neurology*, vol. 15, no. 3, pp. 135–147, 2019, doi: 10.1038/s41582-018-0132-6.

[4]   B. Zeinab and K. Rafikk, "Comprehensive review on Alzheimer'S disease: causes and treatment," *Molecules*, vol. 25, no. 5789, pp. 1–28, 2020.

[5]   F. S. Hanoon and A. H. Hassin Alasadi, "A modified residual network for detection and classification of Alzheimer's disease," *International Journal of Electrical and Computer Engineering (IJECE)*, vol. 12, no. 4, pp. 4400–4407, 2022, doi: 10.11591/ijece.v12i4.pp4400-4407.

[6]   M. Odusami, R. Maskeliūnas, R. Damaševičius, and S. Misra, "Explainable deep-learning-based diagnosis of Alzheimer's disease using multimodal input fusion of PET and MRI images," *Journal of Medical and Biological Engineering*, vol. 43, no. 3, pp. 291–302, 2023, doi: 10.1007/s40846-023-00801-3.

[7]   G. Castellano, A. Esposito, E. Lella, G. Montanaro, and G. Vessio, "Automated detection of Alzheimer's disease: a multi-modal approach with 3D MRI and amyloid PET," *Scientific Reports*, vol. 14, no. 1, 2024, doi: 10.1038/s41598-024-56001-9.

[8]   M. Odusami, R. Maskeliūnas, and R. Damaševičius, "Optimized convolutional fusion for multimodal neuroimaging in Alzheimer's disease diagnosis: enhancing data integration and feature extraction," *Journal of Personalized Medicine*, vol. 13, no. 10, 2023, doi: 10.3390/jpm13101496.

[9]   M. Odusami, R. Damaševičius, E. Milieškaitė-Belousovienė, and R. Maskeliūnas, "Alzheimer's disease stage recognition from MRI and PET imaging data using Pareto-optimal quantum dynamic optimization," *Heliyon*, vol. 10, no. 15, 2024, doi: 10.1016/j.heliyon.2024.e34402.

[10] A. Shukla, R. Tiwari, and S. Tiwari, "Alzheimer's disease detection from fused PET and MRI modalities using an ensemble classifier," *Machine Learning and Knowledge Extraction*, vol. 5, no. 2, pp. 512–538, 2023, doi: 10.3390/make5020031.

[11] R. U. Khan, M. Tanveer, and R. B. Pachori, "A novel method for the classification of Alzheimer's disease from normal controls using magnetic resonance imaging," *Expert Systems*, vol. 38, no. 1, 2021, doi: 10.1111/exsy.12566.

[12] N. Remzan, K. Tahiry, and A. Farchi, "Brain tumor classification in magnetic resonance imaging images using con-

volutional neural network," *International Journal of Electrical and Computer Engineering (IJECE)*, vol. 12, no. 6, pp. 6664–6674, 2022, doi: 10.11591/ijece.v12i6.pp6664-6674.

[13] J. Ramya, B. U. Maheswari, M. P. Rajakumar, and R. Sonia, "Alzheimer's disease segmentation and classification on MRI brain images using enhanced expectation maximization adaptive histogram (EEM-AH) and machine learning," *Information Technology and Control*, vol. 51, no. 4, pp. 786–800, 2022, doi: 10.5755/j01.itc.51.4.28052.

[14] W. Lin, K. Hasenstab, G. Moura Cunha, and A. Schwartzman, "Comparison of handcrafted features and convolutional neural networks for liver MR image adequacy assessment," *Scientific Reports*, vol. 10, no. 1, 2020, doi: 10.1038/s41598-020-77264-y.

[15] Q. Li and M. Q. Yang, "Comparison of machine learning approaches for enhancing Alzheimer's disease classification," *PeerJ*, vol. 9, 2021, doi: 10.7717/peerj.10549.

[16] Q. Zhang, X. L. Yang, and Z. K. Sun, "Classification of Alzheimer's disease progression based on sMRI using gray matter volume and lateralization index," *PLoS ONE*, vol. 17, 2022, doi: 10.1371/journal.pone.0262722.

[17] D. A. Arafa, H. E. D. Moustafa, H. A. Ali, A. M. T. Ali-Eldin, and S. F. Saraya, "A deep learning framework for early diagnosis of Alzheimer's disease on MRI images," *Multimedia Tools and Applications*, vol. 83, no. 2, pp. 3767–3799, 2024, doi: 10.1007/s11042-023-15738-7.

[18] S. Naz, A. Ashraf, and A. Zaib, "Transfer learning using freeze features for Alzheimer neurological disorder detection using ADNI dataset," *Multimedia Systems*, vol. 28, no. 1, pp. 85–94, 2022, doi: 10.1007/s00530-021-00797-3.

[19] Y. AbdulAzeem, W. M. Bahgat, and M. Badawy, "A CNN based framework for classification of Alzheimer's disease," *Neural Computing and Applications*, vol. 33, no. 16, pp. 10415–10428, 2021, doi: 10.1007/s00521-021-05799-w.

[20] W. N. Ismail, F. Rajeena P.P, and M. A. S. Ali, "MULTforAD: multimodal MRI neuroimaging for Alzheimer's disease detection based on a 3D convolution model," *Electronics*, vol. 11, no. 23, p. 3893, Nov. 2022, doi: 10.3390/electronics11233893.

[21] B. Rangaraju, T. Chinnadurai, S. Natarajan, and V. Raja, "Dual attention aware octave convolution network for early-stage Alzheimer's disease detection," *Information Technology and Control*, vol. 53, no. 1, pp. 302–316, 2024, doi: 10.5755/j01.itc.53.1.34536.

[22] E. Tsalera, A. Papadakis, M. Samarakou, and I. Voyiatzis, "Feature extraction with handcrafted methods and convolutional neural networks for facial emotion recognition," *Applied Sciences*, vol. 12, no. 17, Aug. 2022, doi: 10.3390/app12178455.

[23] C. Rajasekhara Rao, M. N. V. S. S. Kumar, G. Sasi, and B. Rao, "Investigation of optimal denoising filter for MRI images," *International Journal of Applied Engineering Research*, vol. 13, pp. 12264–12271, 2018.

[24] N. Rajalakshmi, K. Narayanan, and P. Amudhavalli, "Wavelet-based weighted median filter for image denoising Of MRI brain images," *Indonesian Journal of Electrical Engineering and Computer Science*, vol. 10, no. 1, pp. 201-206, Apr. 2018, doi: 10.11591/ijeecs.v10.i1.pp201-206.

[25] W. T. Freeman and M. Roth, "Orientation histograms for hand gesture recognition," *Gesture*, 1994.

[26] T. Ojala, M. Pietikainen, and D. Harwood, "Performance evaluation of texture measures with classification based on Kullback discrimination of distributions," in *Proceedings of 12th International Conference on Pattern Recognition*, vol. 1, pp. 582–585. doi: 10.1109/ICPR.1994.576366.

[27] T. Ojala, M. Pietikäinen, and D. Harwood, "A comparative study of texture measures with classification based on featured distributions," *Pattern Recognition*, vol. 29, no. 1, pp. 51–59, 1996, doi: 10.1016/0031-3203(95)00067-4.

[28] S. Marĉelja, "Mathematical description of the responses of simple cortical cells," *Journal of the Optical Society of America*, vol. 70, no. 11, p. 1297, Nov. 1980, doi: 10.1364/JOSA.70.001297.

[29] A. K. M. Baareh, A. Al-Jarrah, A. M. Smadi, and G. H. Shakah, "Performance evaluation of edge detection using sobel, homogeneity and prewitt algorithms," *Journal of Software Engineering and Applications*, vol. 11, no. 11, pp. 537–551, 2018, doi: 10.4236/jsea.2018.1111032.

[30] M. M. Hassan, H. I. Hussein, A. S. Eesa, and R. J. Mstafa, "Face recognition based on gabor feature extraction followed by fastica and lda," *Computers, Materials and Continua*, vol. 68, no. 2, pp. 1637–1659, 2021, doi: 10.32604/cmc.2021.016467.

[31] A. Ashraf, S. Naz, S. H. Shirazi, I. Razzak, and M. Parsad, "Deep transfer learning for alzheimer neurological disorder detection," *Multimedia Tools and Applications*, vol. 80, no. 20, pp. 30117–30142, 2021, doi: 10.1007/s11042-020-10331-8.

[32] J. Deng, A. Berg, S. Satheesh, H. Su, A. Khosla, and L. Fei-Fei, "Ilsvrc-2012," 2012. Accessed: Feb 1, 2024. [Online]. Available: https://www.image-net.org/challenges/LSVRC/2012/index.php

[33] M. Bentoumi, M. Daoud, M. Benaouali, and A. Taleb Ahmed, "Improvement of emotion recognition from facial images using deep learning and early stopping cross validation," *Multimedia Tools and Applications*, vol. 81, no. 21, pp. 29887–29917, Sep. 2022, doi: 10.1007/s11042-022-12058-0.

[34] C. Cortes and V. Vapnik, "Support-vector networks," *Machine Learning*, vol. 20, no. 3, pp. 273–297, Sep. 1995, doi: 10.1007/BF00994018.

[35] P. S. Topannavar and D. M. Yadav, "An effective feature selection using improved marine predators algorithm for Alzheimer's disease classification," *International Journal of Electrical and Computer Engineering (IJECE)*, vol. 13,

no. 5, pp. 5126–5134, Oct. 2023, doi: 10.11591/ijece.v13i5.pp5126-5134.

[36] S. T. Ahmed and S. M. Kadhem, "Alzheimer's disease prediction using three machine learning methods," *Indonesian Journal of Electrical Engineering and Computer Science (IJEECS)*, vol. 27, no. 3, pp. 1689–1697, Sep. 2022, doi: 10.11591/ijeecs.v27.i3.pp1689-1697.

[37] B. Charbuty and A. Abdulazeez, "Classification based on decision tree algorithm for machine learning," *Journal of Applied Science and Technology Trends*, vol. 2, no. 1, pp. 20–28, Mar. 2021, doi: 10.38094/jastt20165.

[38] S. T. Ahmed and S. M. Kadhem, "Optimizing Alzheimer's disease prediction using the nomadic people algorithm," *International Journal of Electrical and Computer Engineering (IJECE)*, vol. 13, no. 2, pp. 2052–2067, Apr. 2023, doi: 10.11591/ijece.v13i2.pp2052-2067.

BIOGRAPHIES OF AUTHORS

Touati Menad 🔵 🔢 ⓢⓒ ↻ obtained his M.Sc. degree in electronics from Abdelhamid Ibn Badis University in Mostaganem, Algeria. Currently, he is an assistant professor in the Electrotechnical and Automation Department, Faculty of Science and Technology, Ahmed Zabana University of Relizane, Algeria. His research interests include medical image processing using machine learning and deep learning. He can be contacted at email: touati.menad.etu@univ-mosta.dz.

Mohamed Bentoumi 🔵 🔢 ⓢⓒ ↻ received the engineer degree in electronic from University of Science and Technology of Oran, Algeria, in 1998 and the M.Sc. and Ph.D. degrees in automatic and digital signal processing from University Henri-Poincaré of Nancy, France, in 2000 and 2004, respectively. Currently, he is an associate professor at the Department of Electrical Engineering, Abdelhamid Ibn Badis University of Mostaganem, Algeria. His research interests revolve around the application of machine learning and deep learning techniques in medical image and signal processing, with a specific focus on detection and classification for diagnostic purposes. He can be contacted at email: mohamed.bentoumi@univ-mosta.dz.

Arezki Larbi 🔵 🔢 ⓢⓒ ↻ recieved his master degree in electrical engineering from Abdelhamid Ibn Badis University of Mostaganem in 2017. Currently, he is pursuing his Ph.D. in electronics of embedded systems at the same university. His research interests include EEG, micro-doppler, ECG and EMG signals, application of machine and deep learning on the analysis of physiological signals and time-series forcasting. He can be contacted at email: arezki.larbi@univ-mosta.dz.

Malika Mimi 🔵 🔢 ⓢⓒ ↻ is a professor at Abdelhamid Ibn Badis University of Mostaganem, Algeria. She received B.Sc. in electronics from University of Batna, Algeria in 1985. She obtained her Ph.D. degree in microwave thermography from Department of Physics and Astronomy at Glasgow University, United Kingdom in 1990. Her research activities are focused on medical imaging and signal processing and their applications. She can be contacted at email: mimi_malika2001@yahoo.fr.

Abdelmalik Taleb Ahmed 🔵 🔢 ⓢⓒ ↻ has been a full professor with the Université Polytechnique Hauts-de-France, Valenciennes, France, since 2004. His research interests include segmentation, classification, data fusion, pattern recognition, computer vision, and machine learning, with applications in biometrics, video surveillance, autonomous driving, and medical imaging. Prof. Abdelmalik T. Ahmed has coauthored over 85 peer-reviewed papers and (co)supervised 30 graduate students in these areas of research. He can be contacted at email: abdelmalik.taleb-ahmed@uphf.fr.